UNIVERSIDADE DE SÃO PAULO

INSTITUTO DE FÍSICA
CAIXA POSTAL 66318
05389-970 SÃO PAULO - SP
BRASIL

PUBLICAÇÕES

IFUSP/P-1220

DIFFRACTIVE DISSOCIATION IN THE INTERACTING GLUON MODEL

F.O. Durães and **F.S. Navarra**
Instituto de Física, Universidade de São Paulo

G. Wilk
Soltan Institute for Nuclear Studies, Nuclear Theory Department
ul. Hoża 69, Warsaw, Poland

Maio/1996

Diffractive Dissociation In The Interacting Gluon Model

F.O. Durães[1]*, F.S. Navarra[1,2†] and G. Wilk[2‡]

[1] *Instituto de Física, Universidade de São Paulo*
C.P. 66318, 05389-970 São Paulo, SP, Brazil

[2] *Soltan Institute for Nuclear Studies, Nuclear Theory Department*
ul. Hoża 69, Warsaw, Poland

May 21, 1996

Abstract

We have extended the Interacting Gluon Model (IGM) to calculate diffractive mass spectra generated in hadronic collisions. We show that it is possible to treat both diffractive and non-diffractive events on the same footing, in terms of gluon-gluon collisions. A systematic analysis of available data is performed. The energy dependence of diffractive mass spectra is addressed. They show a moderate narrowing at increasing energies. Predictions for LHC energies are presented.

PACS number(s): 13.85.Qk, 11.55.Jy

In the last years, diffractive scattering processes have received increasing attention for several reasons. These processes may, for example, explain many features of particle production and, in particular, heavy avour production [1] and Centauro events [2]. They are also related to the large rapidity gap physics nd the structure of the Pomeron [3]. In a diffractive scattering, one of the incoming hadrons emerges

*e-mail: dunga@uspif.if.usp.br
†e-mail: navarra@uspif.if.usp.br
‡e-mail: wilk@fuw.edu.pl

from the collision only slightly deflected and there is a large rapidity gap between it and the other final state particles resulted from the other excited hadron. Diffraction is due to the Pomeron exchange but the exact nature of the Pomeron in QCD is not yet elucidated. The first test of a theory (or a model) of diffractive dissociation (DD) is the ability to properly describe the mass (M_X) distribution of diffractive systems, which has been measured in many experiments [4] and parametrized as $(M_X^2)^{-\alpha}$ with $\alpha \simeq 1$. Data presented in [4] were taken at the Tevatron collider ($\sqrt{s} = 1.8$ TeV). They allow us to make comparison with CERN [5] lower energies data and observe the energy dependence of the mass spectrum. In the old Regge theory, the assumption of Pomeron dominance implies that the mass spectrum behaves like $1/M_X^2$ and does not depend on the energy [6] whereas in [4] a slight deviation from this behaviour was reported.

In this work we intend to study diffractive mass distributions using the Interacting Gluon Model (IGM) developed by us recently [7, 8, 9]. In particular, we are interested in the energy dependence of these distributions and their connection with inelasticity distributions [10, 8]. One advantage of the IGM is that it was designed in such a way that the energy-momentum conservation is taken care of before all other dynamical aspects. This feature makes it very appropriate for the study of energy flow in high energy hadronic and nuclear reactions [7, 8, 9] and in cosmic ray studies [10]. In particular, as shown in [8, 9], the IGM was very usefull in analysing data and making predictions on the behaviour of inelasticities and leading particle spectra, including leading charm production [11]. The aim of the present work is to demonstrate that the main characteristics of the DD processes mentioned above emerge naturally from the standard IGM, enlarging profoundly its range of applications.

In Fig. 1 we show schematically the IGM picture of a diffractive dissociation event. According to it (cf. [7, 8, 9] for more details) when two protons collide, their valence quarks fly through essentially undisturbed whereas their gluonic clouds interact strongly with each other (by gluonic clouds we understand a sort of "effective gluons" which include also their fluctuations seen as $\bar{q}q$ sea pairs). One of the protons looses fraction x of its original momentum and gets excited forming what we call a *leading jet* (LJ) carrying $x_L = 1 - x$ fraction of the initial momentum. The other one, which we shall call here the diffracted proton, looses only a fraction y of its momentum but otherwise remains intact [12]. In the standard IGM used previously we were computing the probability $\chi(x, y)$ of depositing energy fractions x and y in the central region in the form of the, so called, (gluonic) *central fireball* (CF) of mass $M = \sqrt{xys}$, which subsequently was decaying and producing particles. Here we shall be rather interested in the mass M_X, a new variable in our problem, which, as can be seen in Fig. 1, is just the invariant mass of a system composed of the CF and leading jet formed by one of the colliding protons (we shall call it also *diffractive mass*). Denoting by E_L and P_L the energy and momentum of the upper (in Fig. 1) proton and by W

and P the energy and momentum of the CF,

$$P_L = E_L = \frac{\sqrt{s}}{2}(1-x), \quad P = \frac{\sqrt{s}}{2}(x-y), \quad W = \frac{\sqrt{s}}{2}(x+y), \tag{1}$$

the energy E_X and momentum P_X of the diffractive cluster are given by:

$$E_X = E_L + W = \frac{\sqrt{s}}{2}(1+y) \quad \text{and} \quad P_X = P_L + P = \frac{\sqrt{s}}{2}(1-y) \tag{2}$$

leading to the following expressions for the mass of our diffractive cluster, M_X, and its rapidity, Y_X:

$$M_X = \sqrt{E_X^2 - P_X^2} = \sqrt{s \cdot y}, \tag{3}$$

$$Y_X = \frac{1}{2}\ln\frac{E_X + P_X}{E_X - P_X} = \frac{1}{2}\ln\frac{1}{y}, \tag{4}$$

where $\sqrt{s}$ is the invariant energy of the pp system. We are working in the cm frame of the incoming nucleons. All masses have been neglected [13].

In the limit $y \to 1$, the whole available energy is stored in M_X which remains then at rest, i.e., $Y_X = 0$. For small values of y we have small masses M_X located at large rapidities Y_X. In order to regard our process as being trully of the DD type we must assume that all gluons from the target proton participating in the collision (i.e., those emitted from the lower vertex in Fig. 1) *have to form a colour singlet*. Only then a large rapidity gap will form separating the diffracted proton (in the lower part of our Fig. 1) and the M_X system (in its upper part), which is the experimental requirement defining a diffractive event. Otherwise a colour string would develop, connecting the diffracted proton and the diffractive cluster, and would eventually decay, filling the rapidity gap with produced secondaries. In this way we are effectively introducing an object resembling closely to what is known as Pomeron ($I\!P$) and therefore in what follows we shall use this notion. Since already some time [14] the Pomeron is treated as being composed of partons, i.e., gluons and sea $\bar{q}q$ pairs, in much the same way as hadrons, with some characteristic distribution functions which will presumably become accurately known in HERA experiments [15].

In our approach the definition of the object $I\!P$ is essentially only kinematical [16], very much in the spirit of those used in all other works which deal with diffractive processes in the parton and/or string language [17, 18, 19, 20]. We shall therefore try to derive the whole M_X^2 dependence directly from the IGM. According to the IGM, the probability to form a fireball carrying momentum fractions x and y of two colliding hadrons is given by:

$$\chi(x,y) = \frac{\chi_0}{2\pi\sqrt{D_{xy}}} \cdot \exp\left\{-\frac{1}{2D_{xy}}\left[\langle y^2\rangle(x-\langle x\rangle)^2 + \langle x^2\rangle(y-\langle y\rangle)^2 - 2\langle xy\rangle(x-\langle x\rangle)(y-\langle y\rangle)\right]\right\}, \tag{5}$$

where

$$D_{xy} = \langle x^2\rangle\langle y^2\rangle - \langle xy\rangle^2$$

and

$$\langle x^n y^m\rangle = \int_0^1 dx\, x^n \int_0^{y_{max}} dy\, y^m\, \omega(x,y), \tag{6}$$

with χ_0 being a normalization factor defined by the condition that

$$\int_0^1 dx \int_0^1 dy\, \chi(x,y)\theta(xy - K_{min}^2) = 1 \tag{7}$$

with $K_{min} = \frac{m_0}{\sqrt{s}}$ being the minimal inelasticity defined by the mass m_0 of the lightest possible CF. In the above expression $y_{max} = \frac{M_X^2}{s}$. This upper cut-off, not present in the usual formulation of the IGM (where $y_{max} = 1$), is our first step necessary to adapt the standard IGM to DD collisions. It is merely a kinematical restriction preventing the gluons coming from the diffracted proton (and forming our object $I\!P$) to carry more energy than the one released in the diffractive system. The, so called, spectral function $\omega(x,y)$ contains all the dynamical input of the IGM in the general form of (cf. [9])

$$\omega(x,y) = \frac{\sigma_{gg}(xys)}{\sigma(s)}\, G(x)\, G(y)\, \Theta\left(xy - K_{min}^2\right), \tag{8}$$

where G's denote the effective number of gluons from the corresponding projectiles (approximated by the respective gluonic structure functions) and σ_{gg} and σ the gluonic and hadronic cross sections, respectively.

We can now calculate the diffractive mass distribution M_X using the $\chi(x,y)$ function by simply performing a change of variables (cf. eq.(3)),

$$\frac{dN}{dM_X^2} = \int_0^1 dx \int_0^1 dy\, \chi(x,y)\, \delta\left(M_X^2 - sy\right)\, \Theta\left(xy - K_{min}^2\right) = \frac{1}{s}\int_{\frac{m_0^2}{M_X^2}}^1 dx\, \chi\left(x, \frac{M_X^2}{s}\right), \tag{9}$$

In the IGM [7, 9] the distribution $\chi(x,y)$ is a wide gaussian in the variables x and y changing slowly with the energy $\sqrt{s}$. Substituting now eq.(5) into eq.(9) we arrive at the following simple expression for the diffractive mass distribution:

$$\frac{dN}{dM_X^2} = \frac{1}{s} \cdot F(M_X^2, s) \cdot H(M_X^2, s) \tag{10}$$

where

$$F(M_X^2, s) = \exp\left[-\frac{\langle x^2\rangle}{2D_{xy}}\left(\frac{M_X^2}{s} - \langle y\rangle\right)^2\right] \tag{11}$$

and

$$H(M_X^2,s) = \frac{\chi_0}{2\pi\sqrt{D_{xy}}}\int_{\frac{m_0^2}{M_X^2}}^1 dx \cdot \cdot \exp\left\{-\frac{1}{2D_{xy}}\left[\langle y^2\rangle(x-\langle x\rangle)^2 - 2\langle xy\rangle(x-\langle x\rangle)\left(\frac{M_X^2}{s}-\langle y\rangle\right)\right]\right\}. \quad (12)$$

The moments $\langle q^n\rangle$, $q = x, y$ and $n = 1, 2$ are given by (6) and are the only place where dynamical quantities like the gluonic and hadronic cross sections appear in the IGM. At this point we emphasize that we are all the time dealing with a proton proton scattering. However, as was said above, we are in fact selecting a special class of events and therefore we must choose the correct dynamical inputs in the present situation, specially the gluon distribution inside the diffracted proton and the hadronic cross section σ appearing in ω. As a first approximation we shall take $G^{I\!P}(y) = G^p(y) = G(y)$ (cf. [14]), with $G(x) = p(m+1)\frac{(1-y)^m}{y}$, with $m = 5$, the same already used by us before [9]. The amount of the diffracted nucleon momentum, p, allocated specifically to the $I\!P$ gluonic cluster and the hadronic cross section σ are both unknown. However, they always appear as a ratio $(\frac{p}{\sigma})$ of parameters in ω and different choices are possible. Just in order to make contact with the present knowledge about the Pomeron, we shall choose

$$\sigma(s) = \sigma^{I\!Pp} = a + b\ln\frac{s}{s_0} \quad (13)$$

where $s_0 = 1\ GeV^2$ and a and b are parameters to be fixed from data analysis. As it will be seen, $\sigma(s)$ turns out to be a very slowly varying function of $\sqrt{s}$ assuming values between 2.6 and 3.0 mb, which is a well accepted value for the Pomeron-proton cross section, and $p \simeq 0.05$.

Before performing a full numerical calculation let us estimate eqs.(10) and (12) keeping only the most singular parts of the gluonic distributions used (i.e., $G(x) \simeq 1/x$) and collecting all other factors in eq.(8) in a single parameter c. Let us first assume that the ratio of the cross sections $\frac{\sigma(xys)}{\sigma(s)}$ does not depend on x and y. Neglecting all terms of the order of $\frac{m_0^2}{s}$ and $\frac{m_0^2}{M_X^2}$ we arrive at the following expressions for the moments calculated in eq.(6):

$$\langle x\rangle = 2\langle x^2\rangle \simeq c\cdot\ln\frac{M_X^2}{m_0^2}; \quad (14)$$

$$\langle y\rangle = 2\frac{s}{M_X^2}\langle y^2\rangle \simeq c\cdot\frac{M_X^2}{s}\cdot\ln\frac{M_X^2}{m_0^2}; \quad (15)$$

$$\langle x\cdot y\rangle \simeq c\left(\frac{M_X^2}{s} - \frac{m_0^2}{s}\cdot\ln\frac{M_X^2}{m_0^2}\right). \quad (16)$$

Notice that in all cases of interest $\langle x\cdot y\rangle$ is much smaller than other moments (by a factor $\ln\frac{M_X^2}{m_0^2}$, at

least). It means that $D_{xy} \simeq \langle x^2\rangle\langle y^2\rangle$ and consequently

$$F(M_X^2,s) \simeq \exp\left[-\frac{\left(\frac{M_X^2}{s}-\langle y\rangle\right)^2}{2\langle y^2\rangle}\right] \simeq \exp\left[-\frac{\left(1-c\cdot\ln\frac{M_X^2}{m_0^2}\right)^2}{c\cdot\ln\frac{M_X^2}{m_0^2}}\right] \quad (17)$$

and

$$H(M_X^2,s) \simeq \frac{\chi_0}{2\pi\sqrt{D_{xy}}}\int_{\frac{m_0^2}{M_X^2}}^1 dx\exp\left[-\frac{(x-\langle x\rangle)^2}{2\langle x^2\rangle}\right] \simeq \text{const}\cdot\frac{\sqrt{\langle x^2\rangle}}{\sqrt{D_{xy}}} = \text{const}\cdot\frac{1}{\sqrt{\langle y^2\rangle}}$$
$$\simeq \text{const}\cdot\frac{s}{M_X^2\cdot\sqrt{c\cdot\ln\frac{M_X^2}{m_0^2}}} \quad (18)$$

leading to

$$\frac{dN}{dM_X^2} \simeq \frac{1}{s}\cdot H(M_X^2,s)\cdot F(M_X^2,s) \simeq \frac{\text{const}}{M_X^2}\cdot\frac{1}{\sqrt{c\cdot\ln\frac{M_X^2}{m_0^2}}}\cdot\exp\left[-\frac{\left(1-c\cdot\ln\frac{M_X^2}{m_0^2}\right)^2}{c\cdot\ln\frac{M_X^2}{m_0^2}}\right]. \quad (19)$$

The expression above is governed by the $\frac{1}{M_X^2}$ term. The other two terms have a weaker dependence on M_X^2. They distort the main $(\frac{1}{M_X^2})$ curve in opposite directions and tend to compensate each other. It is therefore very interesting to note that even before choosing a very detailed form for the gluon distributions and hadronic cross sections we obtain analytically the typical shape of a diffractive spectrum.

In Fig. 2 we show our diffractive mass spectrum and compare it to experimental data from the CERN-ISR [21], which are usually parametrized by the form $\frac{1}{M_X^2}$. These spectra were calculated with expression (10) with gluon distributions and cross sections used in previous works [7, 8, 9]. As it can be seen, the agreement between our curves and data is reasonable. At large values of $\frac{M_X^2}{s}$, experimental points start to flatten out, deviating from the $\frac{1}{M_X^2}$ behaviour. This may be due to the contribution of non-diffractive events. We expect therefore some discrepancy between theory and experiment in this region. Fig. 3 and 4 show similar comparisons for $\sqrt{s} = 546$ and 1800 GeV respectively. Data are from refs. [5] and [4]. Again we find reasonable agreement with experiment. In the low $\frac{M_X^2}{s}$ region at higher $\sqrt{s}$ the agreement is very good. All the curves presented here were obtained with values of parameters in eq. (13) equal to: $a = 2.6$ mb and $b = 0.01$ mb.

As a straightforward extension of our calculation we now apply expression (10) to the study of diffractive pion-proton and kaon-proton scattering. We first consider the cases $p+\pi \to p+X$ and $p+K \to p+X$. This corresponds to replace the proton by a pion or a kaon in the upper line of Fig. 1, everything else remaining the same. We must also substitute the gluon distributions in the proton, $G(x)$, by the corresponding gluon distributions in the pion and kaon, taken from [22]. Here, for simplicity, we take $G^{\pi}(x) = G^{K}(x)$. This is supported by an ACCMOR collaboration data analysis [23]. We also assume that $\sigma^{I\!P p} = \sigma^{I\!P \pi} = \sigma^{I\!P K}$. The comparison between our results and data from the EHS/NA22 collaboration [24] is shown in Figs. 5a (pions) and 5b (kaons). We may also have diffracted mesons, which undergo reactions of the type $\pi + p \to \pi + X$ and $K + p \to K + X$. This corresponds to replace the proton by a pion or a kaon in the lower line of Fig. 1, substituting also the corresponding gluon distributions. The comparison between our results and experimental data [24] is shown in Fig. 6a (pions) and 6b (kaons). As it can be seen, a good description of data is obtained.

We consider now the energy dependence of our results. The CDF collaboration studied single diffractive events and found some energy dependence in the diffractive mass spectrum. This fact is illustrated by writing

$$\frac{s}{\sigma_{SD}} \frac{d\sigma_{SD}}{dM_X^2} \propto \frac{1}{(M_X^2)^{1+\epsilon}} \tag{20}$$

where the factor ϵ which has been reported to be [25] $\epsilon = 0.121 \pm 0.011$ at $\sqrt{s} = 546$ GeV and $\epsilon = 0.103 \pm 0.017$ at $\sqrt{s} = 1800$ GeV, respectively. Considering the error bars one might say that this value is just constant (and that there would be no indication of energy dependence), but a real (albeit small one) change in ϵ is not excluded. Therefore, if confirmed, it would mean that the distribution becomes slightly broader.

In the IGM everything is from the beginning energy dependent and so should be the diffractive mass distribution. We start analysing the analytical approximation, eqs. (10,17, 18). In eq. (18) we see that the s dependence factorizes and the function $H(M_X^2)$ has the same shape for all energies, the difference being only a multiplying factor (in numerical calculations this behaviour is slightly violated). In eq. (17) the s dependence does not factorize and remains in the moments or, equivalently, in the variable c . $F(M_X^2)$ is a broad function with maximum value determined by the moment $\langle y \rangle$ which increases with the energy, making F to "rotate" in a way that it becomes higher at lower values of M_X^2 and becomes deeper at larger values of M_X^2. When we multiply H (which goes essntially like $1/M_X^2$) by F it becomes steeper. This behaviour of F and H is illustrated in Fig. 7a and 7b respectively, which show the numerical evaluation of eqs. (11) and (12). The result of the numerical evaluation of eq. (10) is presented in Fig. 8. There we show the energy dependence of our diffractive mass spectra in proton-proton scattering. Fig. 8a shows diffractive mass spectra for $\sqrt{s} = 23.5$ GeV (solid lines), 44.6 GeV (dashed lines) and 62.4 GeV

(dotted lines). Fig. 8b shows spectra at $\sqrt{s} = 0.54$ TeV (solid lines), 0.9 TeV (dashed lines) and 1.8 TeV (dotted lines). Finally, Fig. 8c shows our prediction for the diffractive mass spectrum at LHC (dashed line) compared to the Tevatron one (solid line). In terms of the parametrization (20), the value of ϵ at $\sqrt{s} = 14$ TeV is 3 % larger than its value at $\sqrt{s} = 1.8$ TeV. The spectra in Fig. 8a and 8b are the same in Figs. 2, 3 and 4. It is interesting to note that the behaviour that we find is not in contradiction with data. In all curves we observe a modest narrowing as the energy increases. This small effect means that the diffractive mass becomes a smaller fraction of the available energy $\sqrt{s}$. In other words, the "diffractive inelasticity" decreases with energy and consequently the "diffracted leading particles" follow a harder x_F spectrum. Physically, in the context of the IGM, this means that the deposited energy is increasing with $\sqrt{s}$ but it will be mostly released outside the phase space region that we are selecting. A measure of the "diffractive inelasticity" is the quantity $\xi = \frac{M_X^2}{s}$. Making a trivial change of variables in eq.(10) we can calculate energy dependence of its average value $\langle \xi \rangle$:

$$\langle \xi(s) \rangle \;\; = \;\; \int_{\xi_{min}}^{\xi_{max}} d\xi \, \frac{dN}{d\xi} \, \xi \tag{21}$$

where ξ_{min} $(= \frac{1.5}{s})$ and ξ_{max} $(= 0.1)$ are the same used in ([25]) for the purpose of comparison. In Fig. 9 we plot $\langle \xi \rangle$ against $\sqrt{s}$. As it can be seen $\langle \xi \rangle$ decreases with $\sqrt{s}$ not only because ξ_{min} becomes smaller but also because $\frac{dN}{d\xi}$ changes with the energy, falling faster. This qualitative behaviour of $\langle \xi \rangle$ is in agreement with the recent estimate of the same quantity extracted from cosmic ray data analysis [26]. Also shown in Fig. 9 is the quantity $\langle \xi^{\epsilon} \rangle$ (which has been discussed in [25] in connection with the energy dependence of the single diffractive cross-section) for $\epsilon = 0.08$ (dashed lines) and $\epsilon = 0.112$ (dotted lines).

The energy behaviour of $\frac{dN}{dM_X^2}$ is determined by the moments (6) and (8). Since $\sigma_{gg}(s)$ and $G(x)$ are the same as in previous works, being thus fixed, the only source of uncertainty in the s dependence of the results is in the ratio $\frac{p}{\sigma}$, which is the only free parameter in the model. All curves presented above were obtained with the choice (13) made for σ (with $a = 2.6$ mb and $b = 0.01$ mb) and with $p \simeq 0.05$. We have checked that for a stronger growth of $\sigma^{I\!P p}$ with $\sqrt{s}$ the energy behaviour of $\frac{dN}{dM_X^2}$ might become even the opposite to that found here, i.e., the diffractive mass distribution would become broader at higher energies. However these strongly s dependent parametrizations do not give an acceptable description of the existing data and were therefore excluded. Considering what was said above one might think that we can discriminate between different Pomeron-proton cross sections and we could use this model to extract $\sigma^{I\!P p}$ from data. We stress however that, in this model, only the ratio $\frac{p}{\sigma}$ enters effectively in the calculations and it is impossible to completely disentangle these two variables. In this sense, the almost constancy (with $\sqrt{s}$) of $\sigma^{I\!P p}$ may be just an indication of some increase of p with $\sqrt{s}$ in a way that the ratio $\frac{p}{\sigma}$ "scales" with the energy.

To conclude, we have shown that:

(*i*) The original IGM ([7, 8, 9]) is reasonably successful in describing non-diffractive events. With only two natural changes, namely the introduction of the kinematical cut-off $y_{max} = \frac{M_X^2}{s}$ and the multiplication of the function ω by a constant factor reflecting the essentially unknown combination of $I\!P$-proton cross section σ and the amount of gluonic energy-momentum of the diffractive proton allocated to the object $I\!P$, p (in form of the ratio $\frac{p}{\sigma}$, with all other parameters kept as in the previous applications of this model) the IGM turns out to be also able to provide a reasonable description of diffractive events [27] and their energy dependence. We predict that, at higher energies, a narrowing of the M_X^2 distribution may be observed.

(*ii*) As is obvious from Fig. 1, IGM provides a detailed description of the diffractive cluster (of mass M_X), *disentangling* it in a natural way into gluonic cluster of mass M containing the majority of produced secondaries (which corresponds to CF in the original IGM) and leading jet (inside the diffractive system) with momentum fraction x_L carrying quantum numbers of the diffractively excited projectile. This fact may be very usefull for the cosmic ray applications of the IGM, in particular to studies using DD like those presented in [2, 28] (where such disentanglement seems to be important and so far was introduced in an *ad hoc* way only).

Acknowledgements: This work has been supported by FAPESP, CNPQ (Brazil) and KBN (Poland). F.S.N. is deeply indepted to his Polish collegaues from SINS, Warsaw, for the hospitality extended to him during his stay there. We would like to warmly thank R. Covolan and Y. Hama for many fruitful discussions.

References

[1] M. Heyssler, "Diffractive Heavy Flavour Production at the Tevatron and the LHC", hep-ph/9602420; A. Bialas and W. Szeremeta,*Phys. Lett.* **B296** (1992) 191; K.Eggert et al. (UA1 Collab.), *Search for diffractive heavy flavour production at the CERN proton-antiproton collider*, in: *Elastic and diffractive scattering*, ed. K.Goulianos, Ed. Frontière, Gif-sur-Yvette, 1988.

[2] R.Attalah and J.N.Capdevielle, *J.Phys.* **G19** (1993) 1381.

[3] J.D.Bjorken, *Nucl. Phys. (Proc. Suppl.)* **B25** (1992) 253.

[4] N.A.Amos et al. (E710 Collab.), *Phys. Lett.* **B301** (1993) 313; F.Abe et al. (CDF Collab.), *Phys. Rev.* **D50** (1994) 5535 (and references therein).

[5] M.Bozzo et al. (UA4 Collab.), *Phys. Lett.* **B136** (1984) 217.

[6] K.Goulianos, *Phys. Rep.* **101** (1983) 169.

[7] G.N.Fowler, F.S.Navarra, M.Plümer, A.Vourdas, R.M.Weiner and G.Wilk, *Phys.Rev.* **C40** (1989) 1219.

[8] F.O.Durães, F.S.Navarra and G.Wilk, *Phys. Rev.* **D50** (1994) 6804 and references therein.

[9] F.O.Durães, F.S.Navarra and G.Wilk, *Phys. Rev.* **D47** (1993) 3049.

[10] Yu.A.Shabelski, R.M.Weiner, G.Wilk and Z.Wlodarczyk, *J. Phys.* **G18** (1992) 1281; Z.Włodarczyk, *J. Phys.* **G21** (1995) 281.

[11] F.O.Durães, F.S.Navarra, C.A.A.Nunes and G.Wilk, *Phys. Rev.* **D53** (1996) in press.

[12] It can be also deflected with some invariant momentum transfer t. However, because the IGM does not include so far any transverse momentum transfers, the results presented here must be regarded as appropriately averaged/integrated over t.

[13] As everywhere in the IGM ([7, 8, 9]) all masses are neglected here. This implies that our approach will be the more accurate the higher is the energy of the reaction and also that it will not be valid for very small values of M_X^2. The IGM is applicable (and was tested) from energies $\sqrt{s} \geq 10$ GeV onward only and this value imposes a lower limit of applicability for the model.

[14] G.Ingelman and P.Schlein, *Phys. Lett.* **B152** (1985) 256; A.Donnachie and P.V.Landshoff, *Phys. Lett.* **B191** (1987) 309; *Nucl. Phys.* **B303** (1988) 634.

[15] M.Derrick et al. (ZEUS Collab.), *Z. Phys.* **C68** (1995) 569 and references therein.

[16] We could therefore (following A.Edin, G.Ingelman and J.Rathsman, *Phys. Lett.* **B366** (1996) 371 and references therein) avoid mentioning the name of Pomeron altogether and treat $I\!P$ as a *preformed colour singlet* object consisting of only a part of the gluonic content of the diffractive proton which is then absorbed by the other proton.

[17] B.R.Desai and U.P.Sukhatme, *Z. Phys.* **C24** (1984) 277.

[18] V.Innocente et al., *Phys. Lett.* **B169** (1986) 285.

[19] L.Lönnblad, *Z. Phys.* **C65** (1995) 285.

[20] J.C.Collins et al., *Phys. Rev.* **D51** (1995) 3182.

[21] M.G. Albrow et at., *Nucl. Phys.* **B108** (1976) 1.

[22] P.J. Sutton, A.D. Martin, R.G. Roberts and W.J. Stirling, *Phys. Rev.* **D45** (1992) 2349.

[23] H. Dijkstra et al. (ACCMOR Collab.), *Z. Phys.* **C31** (1986) 391.

[24] M. Adamus et al. (EHS/NA22 Collab.), *Z. Phys.* **C39** (1988) 301.

[25] K.Goulianos, *Phys. Lett.* **B358** (1995) 379 and references therein.

[26] J. Bellandi, A.L. Godoi, R.J.M. Covolan and J. Montanha, "Diffractive Contribution to the Elasticity and to the Nucleonic Flux in the Atmosphere", Rockefeller University Report RU 96/E-07 (1996).

[27] One should note that we have used in our fits a fair representation of DD data obtained by different groups at different energies and with different set-ups. Because the experimental definition of diffractive events changes from group to group these data are not necessarily consistent with each other. This fact is reflected in the obtained quality of our fits. The older FERMILAB (J.Schamberger et al., *Phys. Rev. Lett.* **34** (1975) 1121 and J.C.Armitage et al., *Nucl. Phys.* **B194** (1982) 365) and ISR (M.G.Albrow et al., *Nucl. Phys.* **B108** (1976) 1) data reporting approximate scaling (i.e., $1/M_X^2$ behaviour) may have some incompatibility with those in [4] and [5] above and they cover only relatively low values of M_X.

[28] Cf., for example, Q.Q.Zhu, L.K.Ding, G.J.Wang and Y.D.He, *J.Phys.* **G20** (1994) 1383 and references therein. We plan to address this problem elsewhere.

Figure Captions

Fig. 1 IGM description of a proton-proton scattering with the formation of a diffractive system of invariant mass M_X.

Fig. 2 Diffractive mass spectrum for pp collisions calculted with the IGM (eq.(9)) and compared with CERN-ISR data [21].

Fig. 3 Diffractive mass spectrum for $p\bar{p}$ collisions calculted with the IGM (eq.(9)) and compared with CERN-SPS Collider data [5].

Fig. 4 Diffractive mass spectrum for $p\bar{p}$ collisions calculted with the IGM (eq.(9)) and compared with FERMILAB Tevatron data [4].

Fig. 5 (a) Diffractive mass spectrum for $p + \pi^+ \to p + X$ collisions calculted with the IGM (eq.(9)) and compared with experimental data [24]. (b) The same as (a) for $p + K^+ \to p + X$ collisions.

Fig. 6 (a) Diffractive mass spectrum for $\pi^+ + p \to \pi^+ + X$ collisions calculted with the IGM (eq.(9) and compared with experimental data [24]. (b) The same as (a) for $K^+ + p \to K^+ + X$ collisions.

Fig. 7 Energy dependences of functions: (a) $F\left(M_X^2, s\right)$ as given by eq. (11); (b) $H\left(M_X^2, s\right)$ as given by eq. (12).

Fig. 8 (a) Energy dependence of diffractive mass spectra calculated with the IGM (eq. (10)). The solid, dashed and dotted lines represent spectra at $\sqrt{s} = 23.5$, 44.6 and 62.4 GeV respectively. (b) The same as in (a) but for $\sqrt{s} = 0.54$ (solid lines), 0.90 (dashed lines) and 1.8 TeV (dotted lines). (c) The same as in (a) but for $\sqrt{s} = 1.8$ (solid lines) and 14 TeV (dashed lines).

Fig. 9 Energy dependence of the "diffractive inelasticity" $\langle \xi \rangle$ and of $\langle \xi^\epsilon \rangle$ discussed in [25].

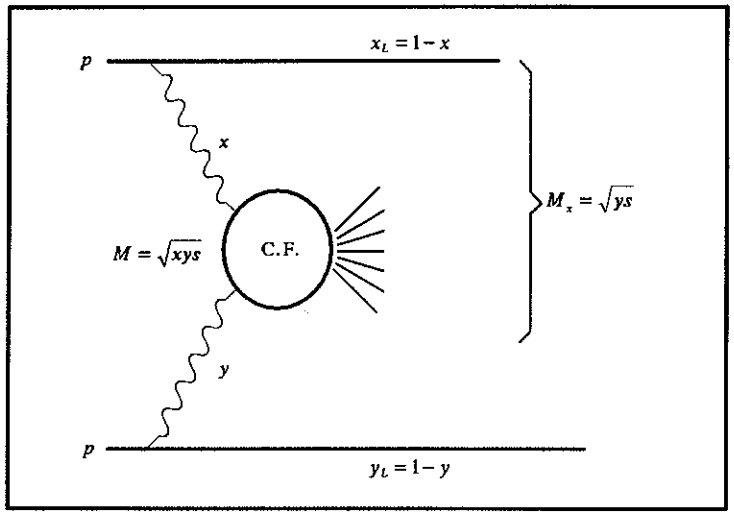

Figure 1

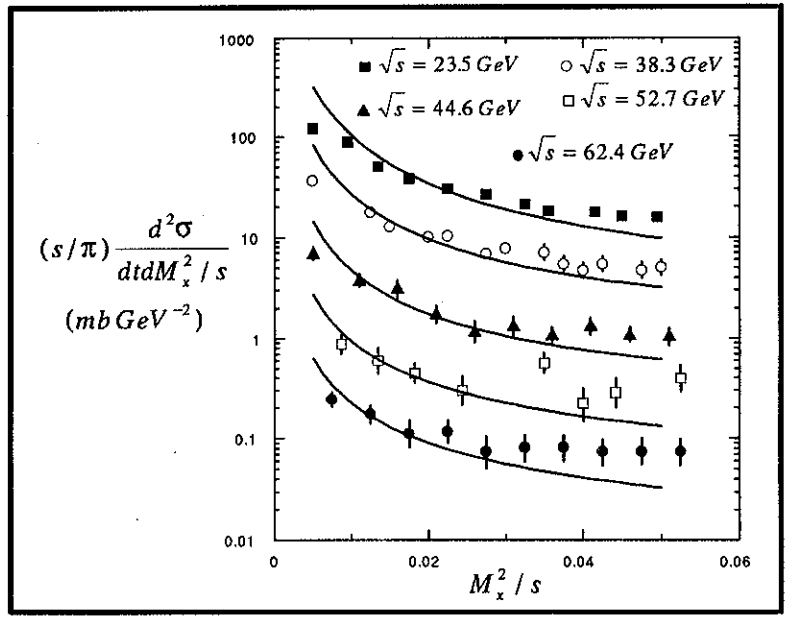

Figure 2

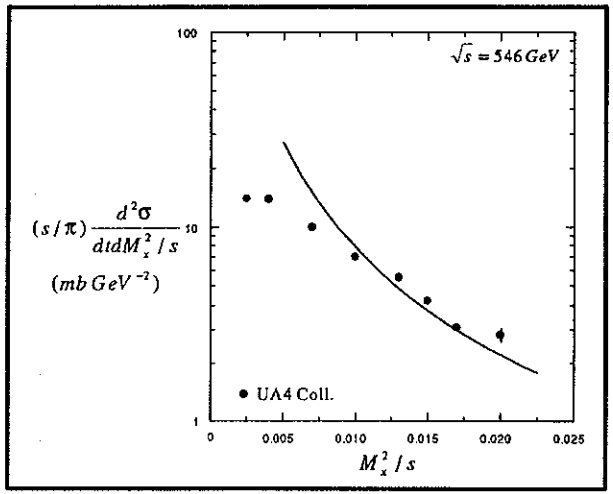

Figure 3

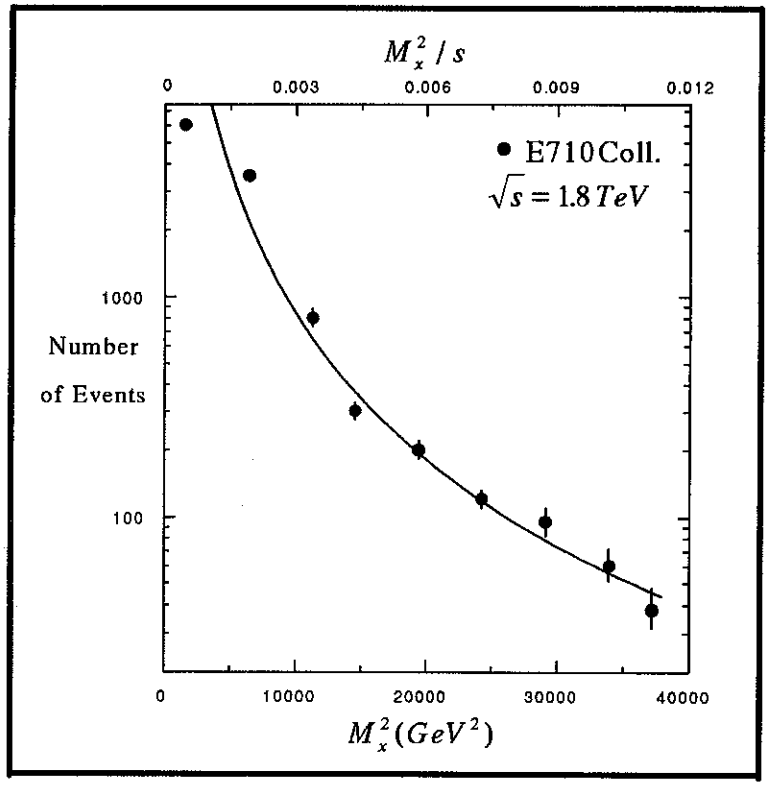

Figure 4

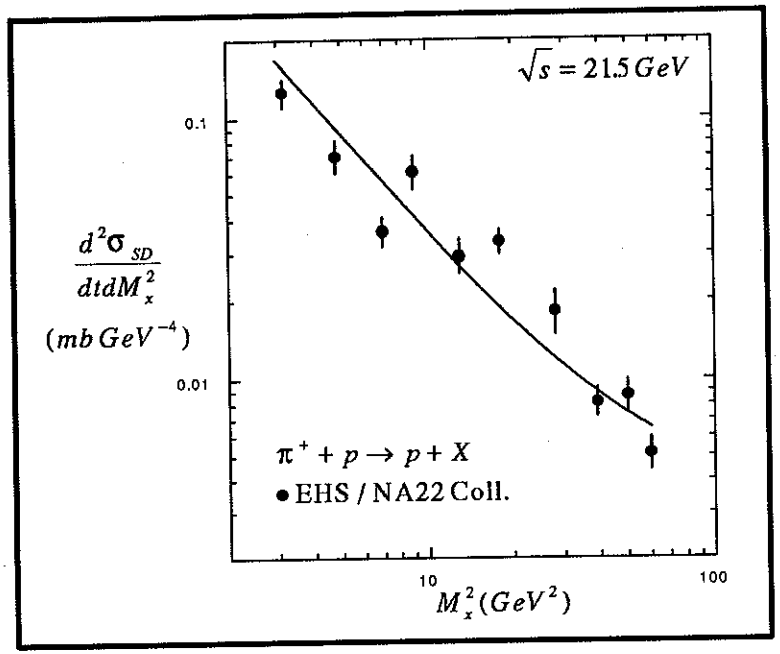

Figure 5a

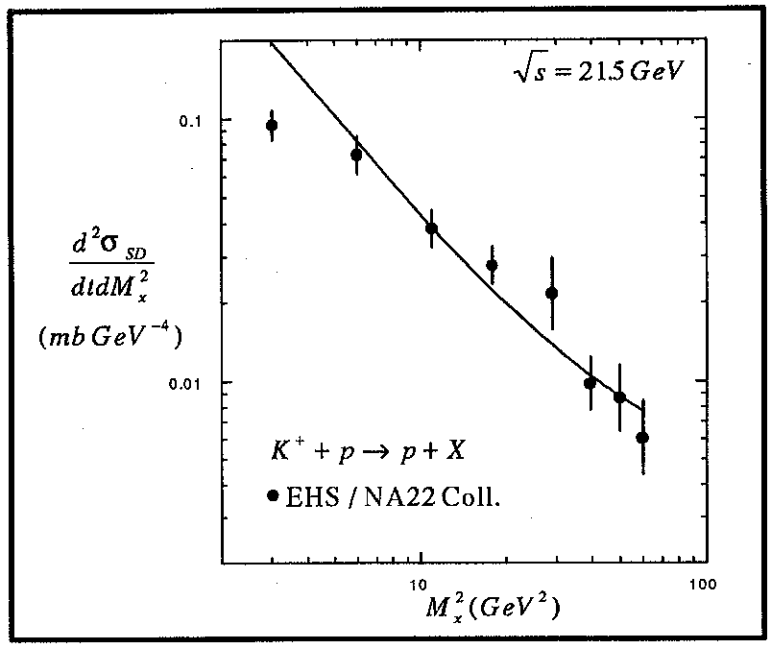

Figure 5b

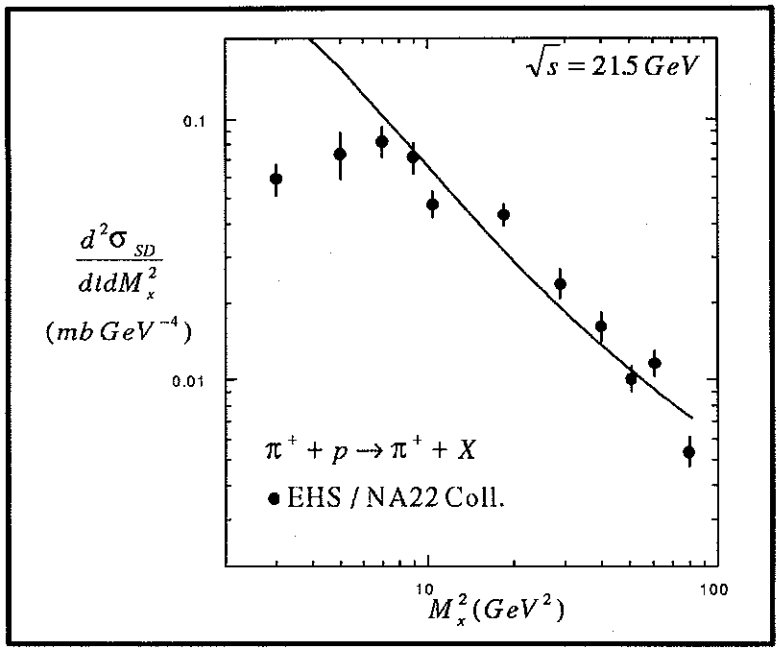

Figure 6a

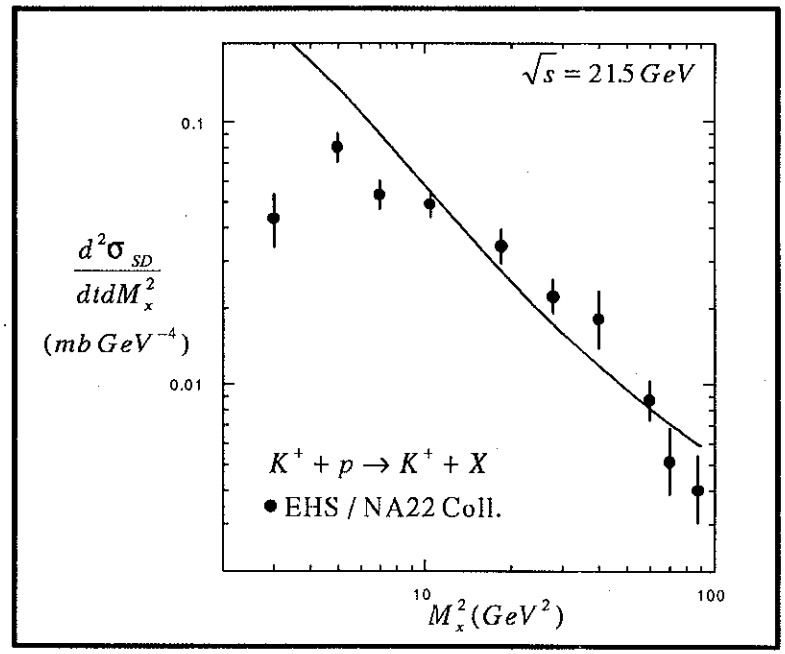

Figure 6b

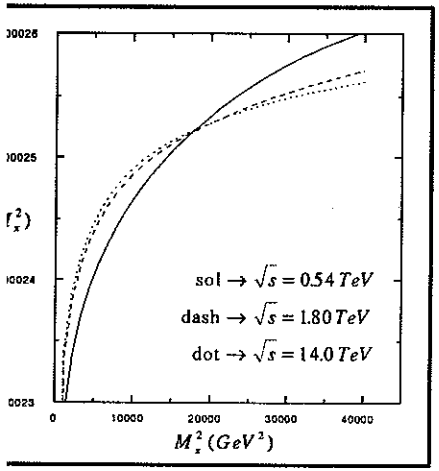

Figure 7a

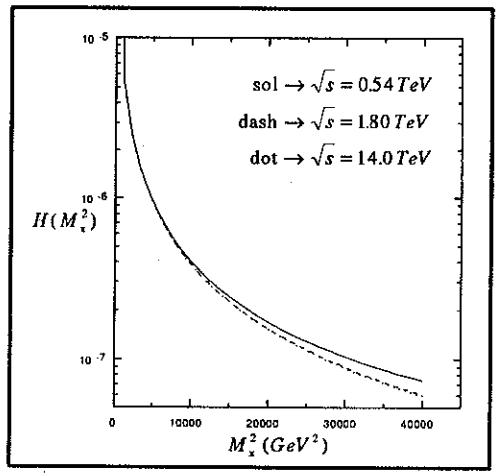

Figure 7b

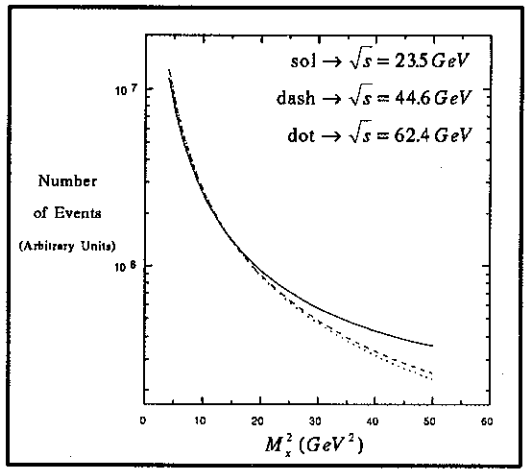

Figure 8a

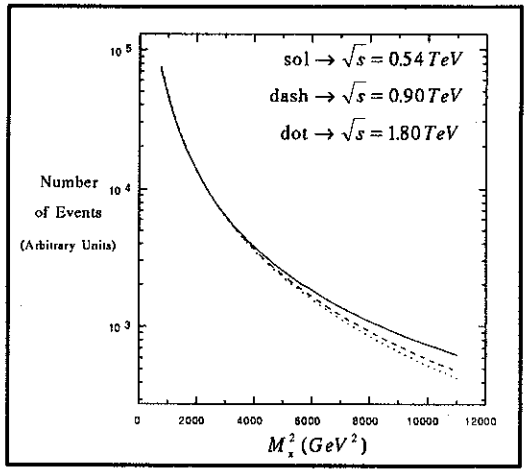

Figure 8b

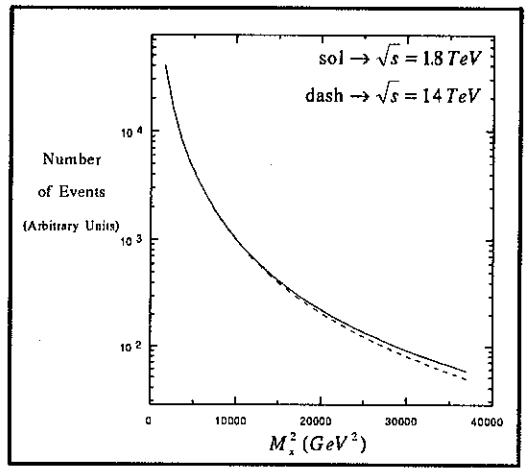

Figure 8c

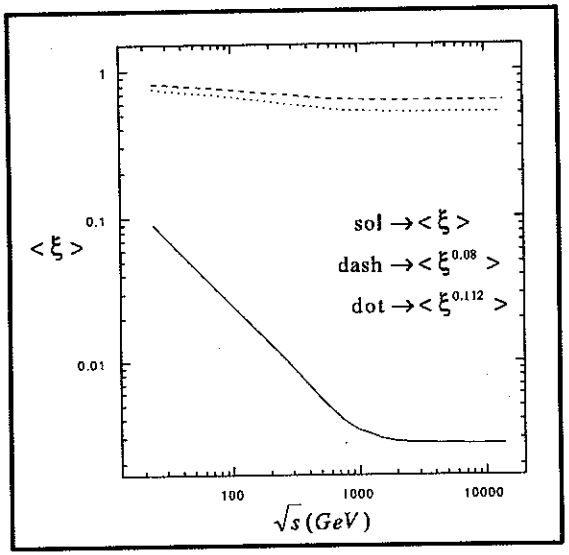

Figure 9